Numerical investigation of the stability of Ag-Cu nanorods and nanowires

Francesco Delogu,[1,*] Elisabetta Arca,[2] Gabriele Mulas,[2] Giuseppe Manai,[3] and Igor Shvets[3]
[1]*Dipartimento di Ingegneria Chimica e Materiali, Università degli Studi di Cagliari, Piazza d'Armi, 09123 Cagliari, Italy*
[2]*Dipartimento di Chimica, Università degli Studi di Sassari, via Vienna 2, 07100 Sassari, Italy*
[3]*School of Physics, Trinity College Dublin, Dublin 2, Ireland*
(Received 22 February 2008; revised manuscript received 9 June 2008; published 8 July 2008)

Molecular dynamics simulations have been employed to investigate thermally-induced phase separation processes in nanometer-sized $Ag_{50}Cu_{50}$ rods and wires. In the absence of concentration gradients, the mechanism underlying the system decomposition consists of two stages. Roughly below 260 K, the thermal response is governed by the displacement of individual surface atoms. Above such temperature, phase separation proceeds via cooperative rearrangements involving also bulklike atomic species. The result is the formation of systems with an Ag-rich phase segregated at the surface. Significantly different thermal responses are obtained in the presence of concentration gradients perpendicular or parallel to the wire axis. First, the phase separation process is favored and takes place at lower temperatures. Second, an almost complete decomposition of the system in Ag- and Cu-rich domains is obtained and not the surface segregation of the Ag-rich phase. The decomposition is also accompanied by a considerable distortion of the originally regular nanowire shape.

DOI: 10.1103/PhysRevB.78.024103 PACS number(s): 64.70.Nd, 81.07.Bc, 82.60.Qr

I. INTRODUCTION

Nanometer-sized systems (NSs) are currently the focus of intense scrutiny due to the impressive suite of novel physical and chemical properties exhibited in contrast to bulk counterparts.[1–3] All such properties can be in principle connected with two fundamental aspects characteristic of NSs.[1–3] First, the fraction of atoms with unsaturated coordination shells is no longer negligible and the rate of surface-involving processes such as self-assembly and catalysis is correspondingly enhanced.[1–3] Second, the number of atoms in NSs is far from the thermodynamic limit.[1–4] The constraints imposed by classical thermodynamics can correspondingly significantly relax, allowing the occurrence of processes unusual for bulk phases.[1–4]

The two above-mentioned factors govern to a various extent the stability of NSs and their capability of withstanding external perturbations. For example, melting points and latent heats of transition have been shown to critically depend on the system size,[1–3,5] decreasing as it decreases.[5] Deformation mechanisms and mechanical properties of NSs such as particles, wires, and tubes are affected as well by size effects.[1–3,6–9] Also the thermodynamic stability of phases is seriously undermined by the dynamics of surface atoms, which are characterized by a significantly larger mobility than bulk atoms. Precisely, this latter general observation takes a particular importance in the case of metastable phases formed by immiscible elements.

The equilibrium phase diagram for immiscible systems in bulk form indicates a very small terminal mutual solubility. The latter is limited to very small atomic percentages as a consequence of the positive enthalpy of mixing.[10] In spite of this, massive crystalline alloys of immiscible elements can still be synthesized by imposing suitable kinetic constraints.[11–13] High cooling rates,[11,12] for example, or the codeformation of metals[13,14] permit one to bypass the tendency to decomposition originating from the positive enthalpy of mixing[5] and keep the elements together in a crystalline lattice. Even though the obtained bulk alloys are expected to be metastable according to equilibrium thermodynamics, they are stable at relatively low temperatures on long time scales.

The aforementioned form of metastability is achieved by the very low mobility of atomic species that prevents, for example, an appreciable growth of local compositional fluctuations. In a bulk system the diffusion paths remain therefore long enough to make decomposition a quite improbable event at relatively low temperatures.[11] In contrast, NSs are characterized by small volumes and the surface atoms possess relatively high mobility.[1–3] It follows that local compositional fluctuations can be unexpectedly amplified, thus originating a structural instability for NSs formed by immiscible elements. The present work aims at investigating precisely this possibility in the case of Ag-Cu NSs by exploiting, in particular, molecular dynamics (MD) methods to analyze their thermal behavior. Ag-Cu represents a classical immiscible system with positive enthalpy of mixing and metastable solubility over the whole compositional range.[5,11,13] Due to the qualitative nature of this study, it should, however, be regarded as a model immiscible system. Attention has been focused first on the role of spontaneous compositional fluctuations. To such an end, the thermal behavior of a small nanometer-sized rod consisting of an equal number of Ag and Cu atoms randomly distributed on the crystalline lattice was characterized. Once the role of spontaneous fluctuations was addressed, attention was shifted to a nanometer-sized wire characterized by concentration gradients along its main axis. It is worth noting that all the NSs dealt with can be in principle prepared via refined solution methods[9–20] and the questions analyzed in this work could be amenable to experimental investigation.

II. MOLECULAR DYNAMICS SIMULATIONS

Reproducing to a satisfactory extent the basic features of metallic systems requires the use of a many-body treatment

TABLE I. Potential parameters for the pure and cross interactions between Ag and Cu atoms.

	A (kJ mol^{-1})	ξ (kJ mol^{-1})	p	q	r_0 (nm)
Ag-Ag	9.936	113.749	10.909	3.141	0.288
Ag-Cu	7.229	107.783	11.000	3.500	0.288
Cu-Cu	8.249	118.099	10.960	2.278	0.255

of interactions, which presents remarkable advantages over the simpler pair-potential description. The so-called Cauchy discrepancy of elastic constants, the estimation of vacancy formation energies and the surface structure, as well as some relaxation properties, can be in such a way better accounted for.[21] This is possible because a many-body potential includes, at least at a phenomenological level, the essential band character of the metallic bond.[21] A relatively simple scheme for relating atomic and electronic structures is represented by the tight-binding (TB) method,[21] which describes the ion-ion interaction by an effective band term and a short-range repulsion. It is based on the evidence that several thermodynamic and structural quantities are mostly related to the average value and effective width of the electron density of states (DOS). The latter is then connected with the crystalline lattice topology via its moments. In particular, the experimental binding energies are proportional to the square root of the second moment, which describes the DOS effective width.[21] An analytic form for the TB potential is obtained by limiting the sum of different electronic contributions to the nearest neighbors.[21] Better performances are, however, obtained by including a larger number of coordination shells.[22] Within the semiempirical TB scheme the cohesive energy is expressed as[22]

$$E = \sum_{k=1}^{N} \sum_{i=\alpha,\beta} s_k^i \left\{ \left[\sum_{l \neq k}^{N} \sum_{j=\alpha,\beta} s_l^j A_{ij} e^{-p_{ij}\left(\frac{r_{kl}}{r_{0,ij}}-1\right)} \right] - \left[\sum_{l \neq k}^{N} \sum_{j=\alpha,\beta} s_l^j \xi_{ij}^2 e^{-2q_{ij}\left(\frac{r_{kl}}{r_{0,ij}}-1\right)} \right]^{1/2} \right\}. \quad (1)$$

The first term on the right-hand side represents a pairwise Born-Mayer repulsive contribution, whereas the second term accounts for the band energy contribution by incorporating a many-body summation.[22] Quantum mechanical in origin, this band energy term approximates the sum of squares of so-called hopping integrals by using an exponential function, rather than the usual power-law dependence of Slater-Koster parameters on the distance r_{kl} between atoms k and l.[22] s_k^i is an occupation variable equal to 1 when the atom k is of species i and 0 otherwise. $r_{0,ij}$ is the distance between nearest neighbors of species i and j at 0 K and N is the total number of atoms. The characteristic parameters A_{ij}, ξ_{ij}, p_{ij}, and q_{ij} quantify the pure and cross interactions between pairs of atoms of chemical species i and j. Their values for Ag-Ag, Cu-Cu, and Ag-Cu interactions were taken from the literature[22,23] and are reported in Table I. Forces were evaluated within a cut-off radius approximately extending to the seventh shell of neighbors.[22,23]

Unsupported nanometer-sized rods roughly 10 nm long with square cross section of about 5 nm in length were generated by starting from a larger bulk system. This contained 64 000 atoms arranged in a crystalline lattice formed by $20 \times 20 \times 40$ elementary crystallographic cells with $cF4$ face-centered-cubic (fcc) symmetry. Ag and Cu atomic species were randomly distributed on the lattice sites to form a metastable equiatomic crystalline solid solution. This system was relaxed within the Nosè-Andersen isobaric-isothermal NPT ensemble with number of atoms N, pressure P, and temperature T constant.[24,25] Temperature and pressure were correspondingly controlled by the Nosè thermostat and the Andersen barostat, which couple the system with heat and stress reservoirs via suitably defined fictitious quantities affecting the dynamics of individual atoms.[24,25] A systematic variation of such quantities for the identification of their best values was carried out in previous work.[22,23] The Parrinello-Rahman scheme was also implemented to properly deal with possible distortions of the elementary cell symmetry.[26] The method essentially regards the side lengths and the angles defining the simulation cell as dynamic variables that can be subjected to significant changes during the course of the simulation, thus allowing the occurrence of possible transitions between phases with different crystallographic symmetry.[26] Equations of motion were solved with a fifth-order predictor-corrector algorithm[27] and a time step of 2 fs. Periodic boundary conditions were applied along the three Cartesian directions. Relaxation was carried out at 200 K and null pressure. Potential and kinetic energy as well as volume fluctuations were monitored to ascertain the attainment of a relaxed configuration. This occurred within about 80 ps, but equilibration was pursued further for an additional 20 ps. Once the bulk was equilibrated in the NPT ensemble, a second relaxation stage of 50 ps was performed in the NVT ensemble with number of atoms N, volume V, and temperature T constant. In this case, the checks for equilibration were carried out also on the fluctuations of the stress levels along the three Cartesian directions.

A parallelepiped-shaped region with the same characteristic sizes of the desired unsupported nanorod was then selected. The parallelepiped orientation with respect to the fcc lattice was suitably chosen in order to form a nanorod of 17 521 atoms with (100) crystallographic facets. The nanorod was finally isolated from the bulk by removing all the atoms outside the parallelepiped. This was done progressively by linearly reducing to zero in 50 ps the A_{ij} and ξ_{ij} potential parameters for the interactions between the atomic species inside and outside the selected region. It is worth noting that, although relatively cumbersome, the described procedure allowed us to obtain remarkably relaxed surfaces.

It should also be noted that the choice of dealing with a nanorod exhibiting (100) facets is motivated by the desire of avoiding difficulties not essential to the qualitative character of the present study. As shown in previous work,[28] most stable wires and rods with fcc lattices are expected to exhibit both (100) and (111) facets. This implies, however, the presence of boundaries along the main axis of the elongated systems, which makes the analysis of the dynamics of individual species more difficult. On the other hand, it is, however, worth noting that the different coordination of atoms in (111) and (100) crystallographic facets is expected to affect their overall mobility. In particular, atoms in the (100) facets should be more mobile than atoms in the (111) facets due to their smaller coordination number.

An analogous procedure was applied to obtain an Ag-Cu nanowire slightly longer than 40 nm with a square cross section of about 5 nm in length and (100) crystallographic facets. In this case, a different bulk system was used consisting of 192 000 Ag and Cu atoms randomly arranged in a crystalline lattice formed by $20\times20\times120$ fcc elementary cells. Such a bulk system was relaxed first in the *NPT* ensemble and then in the *NVT* one for 100 and 50 ps, respectively. The relaxed nanowire contained about 70 000 atoms. Concentration gradients were generated at regular periodic distances along the nanowire axis by ideally dividing the system into eight cubic portions with virtual planes perpendicular to the wire axis. The number of Ag and Cu atoms was changed in the 0.5-nm-wide regions on one side and the other of each virtual plane. More specifically, Ag atoms were randomly selected and transformed into Cu and vice versa. Alternate Ag- and Cu-rich domains were thus created. The 0.5-nm-wide regions were compositionally modified in order to attain at their center the stoichiometries $Ag_{70}Cu_{30}$, $Ag_{80}Cu_{20}$, and $Ag_{90}Cu_{10}$. The overall concentration gradient in Ag-rich domains was then defined case by case by the $Ag_{50}Cu_{50}$ stoichiometry and one of the aforementioned compositions. Concentration gradients in Cu-rich domains were analogously defined by the $Ag_{50}Cu_{50}$ stoichiometry and one of the $Ag_{30}Cu_{70}$, $Ag_{20}Cu_{80}$, and $Ag_{10}Cu_{90}$ compositions. The whole procedure will be detailed in the text when dealing with nanowires characterized by concentration gradients.

Calculations were also performed on a nanowire in which the region characterized by a concentration gradient is parallel to the NS axis. A schematic representation of nanorod and nanowire systems is reported in Fig. 1 for the sake of illustration. The regions involved in concentration gradients are also shown.

The potential parameters employed determine an enthalpy of mixing for the equiatomic $Ag_{50}Cu_{50}$ bulk phase of about +13 kJ mol^{-1}. This value is larger than the experimental one for a chemically-disordered fcc $Ag_{50}Cu_{50}$ bulk solid solution.[10] The difference between predicted and observed values represents in principle a limitation of the TB potential used in this work. A larger positive enthalpy of mixing can, however, be regarded as a significant advantage in the present study. It is indeed expected to enhance the thermodynamic tendency of the alloyed system to decompose, which in turn results in a decrease in simulation times without affecting the qualitative character of the investigation.

The thermal behavior of nanorods and nanowires was studied at null external pressure. The temperature was increased by 2 K every 40 ps. Simulations 20 ns long were also carried out at constant temperature with the aim of characterizing particular aspects of the observed atomic dynamics. Calculations were repeated at least three times to check the reliability of the results obtained.

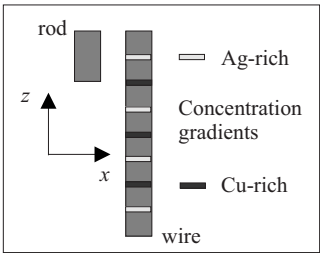

FIG. 1. A schematic representation of the nanorod and nanowire systems investigated. In the latter case concentration gradients along the axis are also indicated for the sake of illustration. The light and dark gray lines indicate, respectively, Ag- and Cu-rich phases.

For each atom, the dynamics was definitely affected by the degree of saturation and geometry of its coordination shell. The increase in the oscillation amplitude actually undergone by the atoms was then dependent on the local arrangement of their nearest neighbors.[29–31] Actually, the species located at edges and surfaces and the ones in the bulklike region of the investigated NSs exhibited different thermal stabilities.

It is worth noting here that two different surface species are considered in the investigated systems, namely, the atoms located at plane surfaces and the ones located at the edges of the regular solid. Surface and edge atoms can be generally distinguished in terms of position and number of nearest neighbors. In different cases the distinction between edge and surface atoms can, however, give rise to misunderstandings and confusion. For this reason, the term "surface atoms" will also be used to include edge atoms. Accordingly, all the atomic species possessing a coordination number smaller than 10 will be referred to as surface atoms.

The mobility of individual atoms was quantified by evaluating their mean square displacement (MSD) $\langle\Delta r^2\rangle$.[27] The self-part of the van Hove function $G_s(l,\Delta t)$ and the nonGaussian parameter $\alpha_2(\Delta t)$ were used to point out the possible occurrence of collective atomic rearrangements.[32,33] The self-part of the van Hove function $G_s(l,\Delta t)$ measures the probability for an atom to cover a distance l in a time interval Δt, whereas the nonGaussian parameter $\alpha_2(\Delta t)$ quantifies the deviation of $G_s(l,\Delta t)$ from a Gaussian distribution. Irrespective of the temperature, the system exhibited a cooperative dynamics on a characteristic time scale τ of about 20–25 ps. Cooperative dynamics was further characterized by evaluating the average number of atoms participating in collective displacements in a time period τ (Refs. 32–34),

$$\bar{n}(\tau)=\frac{\sum n^2P_n(\tau)}{\sum nP_n(\tau)}, \tag{2}$$

where $P_n(\tau)$ represents the probability of observing a group of n atoms undergoing a cooperative rearrangement. Such

atoms were identified on the basis of their mobility, relatively high with respect to the others, and their capability of remaining neighbors after motion has occurred.[32–34] The condition $0.35r_{nn} < |\boldsymbol{r}_i(\tau) - \boldsymbol{r}_i(0)| < 0.86r_{\min}$ was used to identify mobile atoms i. Here $\boldsymbol{r}_i(t)$ represents the ith atom position at time t, r_{nn} is the distance of nearest neighbors indicated by the global pair correlation function (PCF) (Ref. 27), and $r_{\min}$ is the distance at which the global PCF has the first minimum at the temperature considered. Mobile atoms i and j remaining neighbors in correlated displacements were instead defined as the atomic species satisfying the condition $\min[|\boldsymbol{r}_i(\tau) - \boldsymbol{r}_j(0)|, |\boldsymbol{r}_j(\tau) - \boldsymbol{r}_i(0)|] < 0.43r_{nn}$.[34] This condition is based on the assumption, supported by numerical evidence,[34] that in most cases of collective behavior atomic species move in strings. The condition above assures precisely that, after a displacement into the string, the atom i occupies the position formerly occupied by the atom j or vice versa. The displacement length threshold of $0.43r_{nn}$ was chosen to be less than an interatomic distance to distinguish correlated displacements in the string from different mechanism of displacement.[34] The numerical coefficients used are able to effectively separate cooperative motions from thermal vibrations and vacancy-mediated exchanges of atoms.[34] Similar results are obtained when slightly different values are used.

Demixing processes were monitored by evaluating the chemical short-range order (CSRO) parameter[35–37]

$$\Omega = \frac{N_\alpha^\beta + N_\beta^\alpha}{N_\alpha^\alpha + N_\beta^\beta} - 1, \tag{3}$$

where N_α^β (N_β^α) is the average number of nearest neighbors of species β (α) around α (β) atoms. Segregated, randomly mixed, and short-range ordered systems can be thus conveniently identified.[35–37] For such ideal structures the CSRO parameter Ω takes indeed, respectively, the values −1, 0 and 1.

The energy γ_{100} of (100) surfaces of Ag, Cu, and $Ag_{50}Cu_{50}$ alloys was evaluated in simulations carried out in the *NPT* ensemble on a semicrystal according to a procedure described in detail elsewhere.[38] Systems of about 17 100 atoms arranged in stacking sequences of 19 (100) atomic planes were used.

III. DYNAMICS OF INDIVIDUAL ATOMS

The progressive temperature increase determines a corresponding increase in atomic motion. The data shown in Fig. 2 indicate that the MSDs $\langle \Delta r^2 \rangle_{Ag}$ and $\langle \Delta r^2 \rangle_{Cu}$, respectively, of Ag and Cu atoms in the nanowire exhibit a linear dependence on the temperature T. Being almost perfectly superposed to the ones of the nanowire, the data obtained from the nanorod are not shown for the sake of clarity. It appears that the MSDs of atomic species in NSs are on the average significantly larger than the ones of Ag and Cu atoms in massive bulks, also reported in Fig. 2 for comparison. The atoms forming nanorods and nanowires exhibit then a relatively large vibration amplitude.

Such a situation, already reported in literature,[39,40] originates from both structural and thermodynamic factors. The

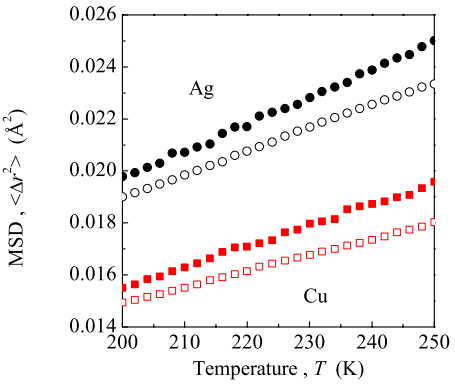

FIG. 2. (Color online) The MSD $\langle \Delta r^2 \rangle_{Ag}$ and $\langle \Delta r^2 \rangle_{Cu}$ of Ag and Cu atoms as a function of the temperature T for the nanowire case (full symbols). The MSD of Ag and Cu atoms in a bulk system are also reported for the sake of comparison (open symbols).

former can be suitably pointed out by classifying the atoms in the NSs investigated as a function of their MSDs. The evaluation and comparison of the MSD values of individual Ag and Cu atomic species indicate that three different sets of atoms can be identified on such basis. The MSD values characteristic of each set are reported in Fig. 3 for Ag and Cu atoms in the nanorod system as a function of their average potential energy u. This is defined as the average potential energy of the central atom interacting with all the neighboring species located within the potential cut-off radius. Analogous data are obtained in the case of nanowires. It can be seen that the larger MSD values pertain to Cu atoms located at the edges of the nanorod. Intermediate MSD values are instead characteristic of atoms located at the plane (100) surfaces, whereas the smallest ones pertain to species located in the bulklike region. The term "bulklike" is in this context motivated by the evidence that the MSD of bulklike species is approximately equal to the one of Ag and Cu atoms in a massive bulk at the same temperature, as can be seen by comparing the data reported in Figs. 2 and 3. The hierarchy of MSD values observed thus reveals that the vibration amplitude, and in a sense the mobility, of Ag and Cu atoms

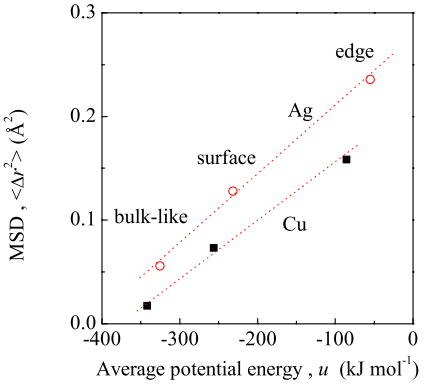

FIG. 3. (Color online) The characteristic MSD $\langle \Delta r^2 \rangle_{Ag}$ and $\langle \Delta r^2 \rangle_{Cu}$ values worked out from the analysis of individual Ag and Cu atom dynamics as a function of their average potential energy u. Data refer to the nanorod case at 254 K. The atomic sets from which the values originate are also indicated.

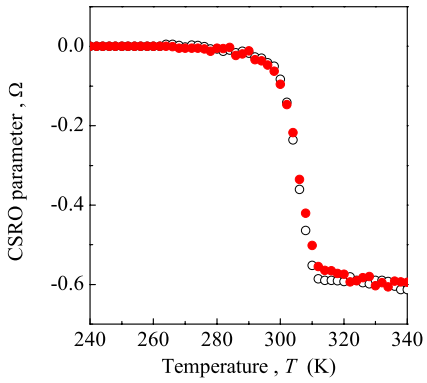

FIG. 4. (Color online) The CSRO parameter Ω of the nanorod (open circles) and nanowire (full circles) systems with no concentration gradient as a function of the temperature T.

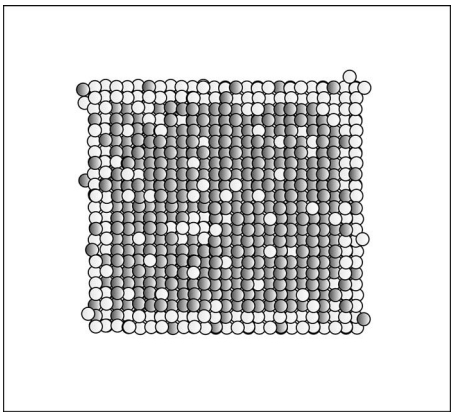

FIG. 5. The cross-sectional view of the nanorod at 312 K. The light and dark gray circles indicate, respectively, Ag and Cu atoms.

roughly scales with the number of coordinated species. It is the different coordination number that determines the different thermal response of edge, surface, and bulklike atoms. It thus represents a fundamental feature to understand the dynamics of atomic species in NSs.

The thermal response of the investigated NSs is also affected by thermodynamic factors, which are though much less important than structural ones. Their existence can be pointed out by comparing the MSD values for Ag and Cu atoms located in their pure bulks and in a $Ag_{50}Cu_{50}$ bulk system. It appears in fact that Ag and Cu bulklike atoms in the systems investigated, as well as the ones in a disordered $Ag_{50}Cu_{50}$ bulk alloy, exhibit MSD values about 10% larger than Ag and Cu atoms in pure Ag and Cu lattices at the same temperature. The larger amplitude of atomic motion of bulklike species in alloyed systems can be in first approximation related to the unfavorable potential energy of cross Ag-Cu interactions with respect to pure Ag-Ag and Cu-Cu ones. The positive enthalpy of mixing induces indeed a tendency toward spontaneous decomposition of the metastable alloy, which, in turn, can be thought to enhance the atomic mobility.

The different features discussed above are common to the nanorods and nanowires investigated. However, the thermal response of each system is intimately connected with its structural and thermodynamic characteristics. This means that the nanorod and the nanowire with no concentration gradient along the axis are expected to exhibit a thermal behavior different from the one of nanowires with concentration gradients. For the sake of clarity, the two different cases will be thus discussed separately.

IV. NANOROD AND NANOWIRE WITH NO CONCENTRATION GRADIENT

The nanorod and the nanowire, respectively, 10 and 40 nm long exhibit a similar thermal response, which was studied by monitoring the variation of the CSRO parameter Ω with the temperature T. The data for the two systems are shown in Fig. 4. In both cases, the first indications of system decomposition are detected at about 266 K, when Ω starts a gradual decrease from 0 to negative values. Phase segregation processes occur correspondingly and 266 K can be regarded as the temperature for the onset of decomposition. The Ω decrease proceeds at low rates until a temperature of about 298 K is attained. A drop of Ω values from roughly −0.06 to −0.59 is then observed between 298 and 312 K. At 312 K the nanorod and nanowire systems are characterized by a considerable segregation degree, with an Ag-rich phase separated by a Cu-rich one. The cross-sectional views of the nanorod and nanowire at 312 K, one of which is presented in Fig. 5 for the sake of illustration, clearly show that the Ag-rich phase has segregated at the system surface. It is, however, worth noting that the structures with the Ag- and the Cu-rich phases, respectively, at the surface and in the bulk have undergone only a partial decomposition. Their compositions correspond in fact to about $Ag_{80}Cu_{20}$ and $Ag_{20}Cu_{80}$.

The occurrence of surface segregation phenomena in Ag-Cu binary immiscible NSs is a well-known fact.[41,42] The phase separation process promotes the formation of the NSs with the lowest possible surface energy. Therefore surface energies play a major role and the results can be sensitive to the capability of the force scheme employed in reproducing the surface properties. In the specific case of the TB potential, the surface energy γ values predicted for (100), (110), and (111) surfaces for Ag, Cu, and disordered $Ag_{50}Cu_{50}$ systems are reported in Table II. The corresponding surface energy γ values obtained from *ab initio* calculations[43] are also reported for the sake of comparison. It can be seen that, although smaller than *ab initio* ones, the surface energy γ values obtained from TB potential follow the same hierarchy. The γ values for the systems considered here are therefore reliable at least on a relative basis, which is the necessary level of accuracy required to the present qualitative work. It appears that the energy γ_{100} of Ag (100) surfaces is lower than the one of Cu and $Ag_{50}Cu_{50}$ surfaces. The Ag surface segregation processes in nanorods and nanowires determine then the formation of the most stable segregated phases. A decomposed system with the Cu-rich phase at the surface would indeed have a remarkably higher surface energy.

As the temperature further increases above 312 K a corresponding increase in the degree of phase separation is observed. The decrease in the CSRO parameter Ω is, however, quite slow and values around −0.80 are attained only at

TABLE II. The energy γ values for (100), (110) and (111) surfaces for Ag, $Ag_{50}Cu_{50}$ and Cu systems as obtained from TB potential (upper panel). The energy γ values for (100), (110) and (111) surfaces for Ag and Cu systems as obtained from *ab initio* calculations (lower panel).

TB potential	Ag	$Ag_{50}Cu_{50}$	Cu
γ_{100}, Jm^{-2}	0.98	1.34	1.53
γ_{110}, Jm^{-2}	1.07	1.42	1.63
γ_{111}, Jm^{-2}	0.86	1.13	1.37
Ab initio[a]	Ag	Cu	
γ_{100}, Jm^{-2}	1.29	1.93	
γ_{110}, Jm^{-2}	1.42	2.04	
γ_{111}, Jm^{-2}	1.14	1.73	

[a]Reference 41.

about 500 K. Being Ω still around −0.86 at about 900 K, no significant dynamical event takes place below such temperature except for atomic displacements promoting a very slow demixing process. This slow transformation is replaced by a significantly faster dynamics roughly above 920 K, when a premelting process involves the surface layers of both nanorod and nanowire systems. In correspondence with the aforementioned temperature range a rise in the CSRO parameter Ω values is observed. Surface premelting induces indeed a mixing of the Ag and Cu chemical species, which are miscible in the liquid phase. Being only the outer surface layers involved by premelting, a limited Ω increase is observed. Complete mixing is instead attained above 942 K, when melting also involves the bulklike region. This determines the interdiffusion of elements as a consequence of the relatively fast dynamics of the liquid phase.

The phenomenological description of the thermal behavior of nanorod and nanowire systems deserves a further comment here. The mechanistic scenario described above is indeed sensitive to the rate at which the temperature is gradually raised. More specifically, the temperatures at which the various characteristic steps of the decomposition process take place are expected to decrease as the heating rate decreases and vice versa. These are of course changes of quantitative nature. Qualitative changes are not expected.

A. Mechanism of phase separation

As shown by the CSRO parameter Ω data discussed above, the alloy decomposition proceeds gradually. At least two different stages, characterized by different atomic mobility regimes, can be identified depending on the temperature range. Although according to the Ω values decomposition starts approximately at 266 K, a careful analysis of atomic displacements points out that local phase separation processes involve surface layers already at about 250 K. This can be ascribed to the enhanced mobility of edge and surface atoms. Edge atoms, in particular, undergo relatively long-range displacements even at temperatures below 256 K. Exhibiting an apparently stochastic dynamics, edge atoms are not only capable of moving along the edges of NSs, but also

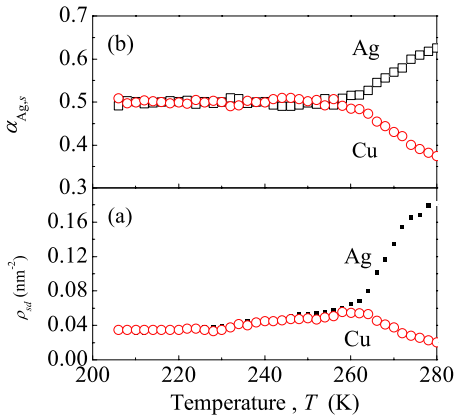

FIG. 6. (Color online) (a) The number densities $\rho_{Ag,sd}$ and $\rho_{Cu,sd}$ of Ag and Cu surface domains and (b) the fractions $\alpha_{Ag,s}$ and $\alpha_{Cu,s}$ of Ag and Cu surface atoms as a function of the temperature T.

of exploring the adjacent plane surfaces. Under such circumstances, they behave like adsorbed species diffusing over the two-dimensional surface domain. It is precisely during such events that edge atoms occasionally exchange their position with atomic species of the underlying surface. Thus, an atom originally located at the edge of the nanorod or the nanowire becomes a surface species. At the same time, the opposite process occurs and a surface atom transforms into an adsorbed species and starts its thermal diffusion on the plane surface.

All the atomic exchange events observed during this stage are remarkably localized and involve only two species. No evident indication of collective character was obtained. It seems that exchanges are aimed at increasing the number of neighboring atoms of the same species, thus establishing the highest possible number of pure favorable Ag-Ag or Cu-Cu interactions. In fact, exchanges hardly involve atoms of the same chemical species. In other words, adsorbed Ag (Cu) atoms exchange their positions with surface Cu (Ag) atoms and not with Ag (Cu) ones.

The progressive replacement of surface atoms of a given species with atoms of the other determines the formation at plane surfaces of pure Ag and Cu domains. The number N_{sd} of such domains for Ag and Cu species was roughly estimated by identifying the surface regions in which a given Ag (Cu) atom has at least five Ag (Cu) nearest neighbors also located at the surface. At temperatures below 260 K the Ag and Cu surface islands form with approximately the same probability. This can be seen from Fig. 6(a), where the number densities $\rho_{Ag,sd}$ and $\rho_{Cu,sd}$ of Ag and Cu surface domains per surface area unit are reported as a function of the temperature T. The $\rho_{Ag,sd}$ and $\rho_{Cu,sd}$ values are indeed roughly equal. The two quantities become instead increasingly different at temperatures above 260 K. In particular, the number density $\rho_{Ag,sd}$ of Ag domains increases, whereas the $\rho_{Cu,sd}$ one of Cu domains decreases. This indicates that Ag surface domains are formed preferentially. A behavior similar to the one of $\rho_{Ag,sd}$ and $\rho_{Cu,sd}$ quantities is exhibited by the fractions $\alpha_{Ag,s}$ and $\alpha_{Cu,s}$ of Ag and Cu surface atoms, defined respectively as the ratio between the number of Ag or Cu surface atoms and the total number of atoms in the system. The $\alpha_{Ag,s}$

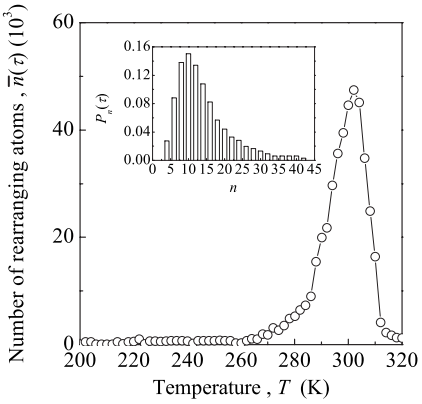

FIG. 7. The average number $\bar{n}(\tau)$ of atoms undergoing collective rearrangements as a function of the temperature T. The inset shows the probability $P_n(\tau)$ of finding a cluster of n mobile atoms in a time period τ. Data refer to the case of the nanorod at 270 K.

and $\alpha_{\mathrm{Cu},s}$ data are shown in Fig. 6(b) as a function of the temperature T. Initially almost coincident, $\alpha_{\mathrm{Ag},s}$ and $\alpha_{\mathrm{Cu},s}$ also begin to change above 260 K, with $\alpha_{\mathrm{Ag},s}$ increasing with temperature T. The increase in $\alpha_{\mathrm{Ag},s}$ proceeds monotonically until the whole surface is formed by Ag atoms. It is worth noting that the continuous increase in the number of Ag surface atoms is eventually responsible for the decrease in the number density $\rho_{\mathrm{Ag,sd}}$ of Ag surface domains. It determines indeed first their growth and then their coalescence.

The preferential formation of Ag surface domains above 260 K suggests a change of the mechanism underlying atomic displacements. In fact, the segregation of Ag atoms at the surface necessarily implies the involvement of bulklike species in atomic rearrangements. It represents in fact the only possibility of increasing the number of Ag atoms at the surface. The change of mechanism must be ascribed to the fact that while individual atoms can easily exchange their position as far as only surface species are involved, cooperative processes are required in the case of more complex rearrangements involving bulklike species.

The mobility of Ag and Cu atoms in this stage was characterized by means of the self-part of the van Hove function $G_s(l,\Delta t)$. The $G_s(l,\Delta t)$ functions of both the Ag and Cu atomic species exhibited a second peak approximately at the average distance $r_{nn,\alpha\alpha}$ of nearest neighbors indicated by the partial $\alpha\alpha$ PCFs. Such a peak underwent a relatively slow growth, attaining a maximum value after a time period τ of about 25 ps. The time period τ is roughly the same for Ag and Cu species. At the same time period τ the nonGaussian parameter $\alpha_2(\Delta t)$ also attained a maximum. According to previous work,[32,33] such evidences were ascribed to the occurrence of cooperative diffusion processes.

The transition between two atomic mobility regimes at about 260 K is further demonstrated by the data concerning the number of atoms participating in collective displacements on time scales measured by τ. The average number $\bar{n}(\tau)$ of collectively rearranging atoms is reported in Fig. 7 as a function of temperature T. Data indicate that $\bar{n}(\tau)$ values are very small at temperatures below 260 K, whereas a progressive increase is observed above it. It follows that individual atomic displacements taking place during the first stage of phase separation at temperatures below 260 K are gradually replaced by cooperative rearrangements. A maximum value is attained slightly above 300 K, followed by a rapid decrease to zero above 320 K. This indicates that the temperature range over which cooperative rearrangements effectively occur is quite limited. The rationale for such behavior is provided by the fact that collective atomic displacements take place as far as Ag surface segregation is not completed. With the partial decomposition complete at about 320 K, as indicated by the CSRO parameter Ω data in Fig. 4, cooperative rearrangements are correspondingly no longer observed.

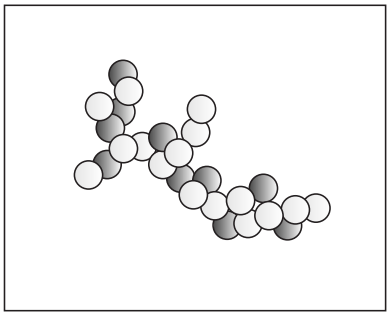

FIG. 8. A cluster of mobile Ag and Cu atoms. The cluster was taken from an atomic configuration of the nanorod at 268 K. The light and dark gray circles indicate, respectively, Ag and Cu atoms.

It is worth noting here that only the $\bar{n}(\tau)$ values mark the occurrence of the aforementioned transition. The probability $P_n(\tau)$ of finding a cluster of n mobile atoms in a time period τ, shown in the inset of Fig. 7 for the temperature of 270 K, exhibits indeed the same shape irrespective of the temperature. The average chemical composition of mobile atom clusters is left unaffected in an analogous way. Such average composition corresponds to the relative number of Ag and Cu species participating in correlated displacements. Independent of temperature, a cluster of n mobile atoms is formed on the average by about 0.52 n Ag and 0.48 n Cu atoms. It follows that Ag and Cu atoms exhibit in cooperative rearrangements roughly the same atomic mobility.

One of the relatively large clusters formed by mobile Ag and Cu atoms is shown in Fig. 8 for the sake of illustration. Such clusters have a disordered structural arrangement resembling the one of fractal aggregates. The dimensionality of clusters with number of connected atoms n larger than ten was estimated by approximately quantifying their average fractal dimension d_f. This was done by identifying the two most distant atoms within each cluster and evaluating their distance, which is generally referred to as the cluster length L.[44] The logarithm of L, ln L, was then plotted as a function of the logarithm of the cluster size n, ln n. The data, quoted in Fig. 9, exhibit an approximately linear arrangement with slope ν. It follows that L and n obey the power law $L \propto n^{\nu}$. Once evaluated the average slope ν by carrying out a linear best-fitting of data, the average fractal dimension d_f was finally estimated by taking advantage of the relationship $\nu \approx d_f^{-1}$.[44] A d_f value of about 1.23 was obtained. It thus appears that the mobile atom clusters formed in the regime of cooperative atomic mobility tend to a one-dimensional occu-

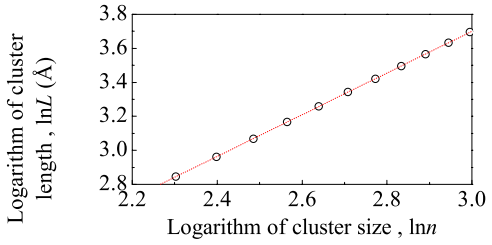

FIG. 9. (Color online) The logarithm of L, ln L, as a function of the logarithm of n, ln n. A best-fitted line with slope ν is also shown. Data refer to the nanorod at 300 K.

pancy of space. They have a stringy arrangement and can be thought as roughly connecting the surface of the nanorod and nanowire systems with their interiors. Such an arrangement promotes the exchange of atomic species between the two regions and permits the involvement of bulklike atoms in cooperative rearrangements.

The formation of mobile atom clusters and the cooperative character underlying atomic mobility at temperatures above 260 K determine a relatively fast evolution of the NS structures. The CSRO parameter Ω values point out that the phase separation processes mediated by highly cooperative atomic rearrangements terminate at about 312 K, when not all the Ag atoms have segregated at the surface. The observed arrest of the decomposition reaction is due to the consumption of the Ag atoms in the layers immediately below the surface. Such a phenomenon, responsible for the enrichment in Cu atoms of the layers immediately below the surface, has been already observed and reported in literature.[45] Under such conditions, the Ag atoms should reach the surface by diffusion starting from the bulklike interior. Correspondingly, their arrival at the surface is much slower. In addition, the diffusion mechanism also changes. Cooperative rearrangements are indeed replaced by conventional, vacancy-mediated thermal diffusion processes. This is probably due to the fact that phase decomposition can be considered almost complete in the surface regions and in their neighborhoods. For this reason, the chemical driving force related to the positive enthalpy of mixing has essentially disappeared. Under such circumstances, the atomic mobility is mostly restricted to edges and surfaces until temperatures as high as 750 K are reached. It is finally worth noting that the MSD values exhibited by both Ag and Cu atoms are smaller at this stage than during the initial stages of the phase separation process. This can be once more rationalized by invoking a sort of dynamical arrest consequent to demixing. Reducing the thermodynamic metastability, the partial system decomposition has also reduced the atomic mobility.

B. Long-time behavior at constant temperature

The stability of the nanorod against phase decomposition was also investigated in simulations about 20 ns long at constant temperature. Two temperatures were selected in order to characterize the system behavior under the two identified atomic mobility regimes. Calculations were thus carried out at 256 and 278 K starting from atomic configurations attained in simulations performed under gradual heating conditions. An additional test was performed on a nanorod in which a given number of Ag and Cu atoms were selected and removed to create vacancies. The structural and chemical evolution of the nanorod was then followed as in the other cases to ascertain the role of vacancies in the phase separation process.

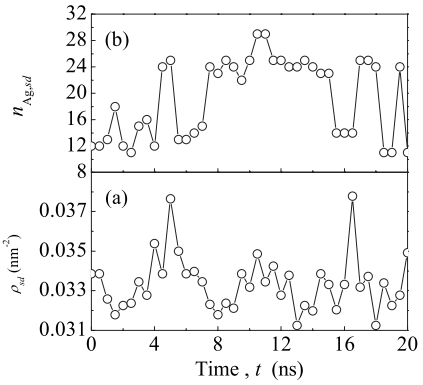

FIG. 10. (a) The number density $\rho_{Ag,sd}$ of Ag surface domains and (b) the number $n_{Ag,sd}$ of atoms connected in a single Ag surface domain cluster as a function of the time t. Data refer to the nanorod at 256 K.

Three simulations were carried out at 256 K. The first two indicate that the demixing process does not proceed after the stage in which Ag and Cu surface domains are formed. The mobility of atomic species located at the edges and plane surfaces permits the nucleation and growth of such domains, but the structural evolution attains a dynamic equilibrium between the formation of new domains and the disappearance of old ones. This can be seen from Fig. 10(a), where the number density $\rho_{Ag,sd}$ of Ag surface domains is reported as a function of the time t. In fact, $\rho_{Ag,sd}$ undergoes continuous and significant fluctuations roughly between 15 and 30. Such fluctuations originate from the coalescence and decoalescence of neighboring surface domains as a consequence of the dynamics of individual atoms. The influence of such dynamics on the number density and size of surface domains can be indirectly inferred from the data shown in Fig. 10(b), where the size $n_{Ag,sd}$ of a given Ag surface domain is reported as a function of the time t. Data indicate that the number $n_{Ag,sd}$ of Ag atoms connected in the surface cluster changes irregularly and discontinuously over time intervals shorter than the time period τ characteristic of cooperative motion. The time scale observed in this case is therefore regarded as characteristic of the individual atom dynamics. It can be seen that the number n of connected atoms not only undergoes small changes amounting to single units, but also significant changes of 10 to 20 units. These are related to the coalescence or decoalescence of relatively large surface domains.

In the third simulation carried out at 256 K the nanorod exhibited a particular structural evolution. During the first 4 ns the dynamics of atomic species did not show significant differences with respect to previous cases. However, already at 5 ns a particularly high concentration of Ag atoms was observed at one of the nanorod vertices. The detailed analyses performed successively pointed out that the motion of

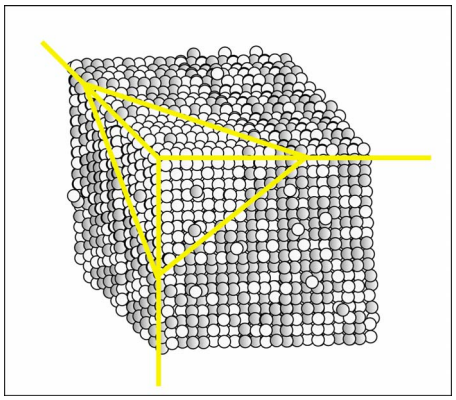

FIG. 11. (Color online) The atomic configuration of the nanorod in the neighborhood of the Ag-rich vertex after about 14 ns from the beginning of the simulation at 256 K. The light and dark gray circles indicate Ag and Cu atoms, respectively. The nanorod edges are also marked together with the approximate boundaries of the Ag-rich vertex.

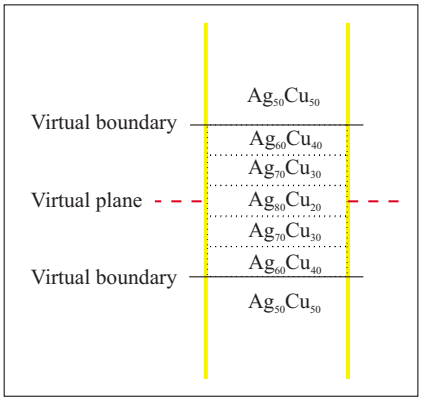

FIG. 12. (Color online) A schematic representation of a concentration gradient along the nanowire axis. The boundary and virtual planes perpendicular to the wire axis are also shown. The boundary planes identify the 1-nm-wide zone containing the concentration gradient. The case refers to a central domain with $Ag_{80}Cu_{20}$ composition.

edge and surface atoms locally produced a significant deviation from the equiatomic $Ag_{50}Cu_{50}$ stoichiometry. Actually, a slight deviation from such stoichiometry was already present at the beginning of the simulations. The ratio of Ag to Cu atoms was indeed equal to about 55 to 45. This is true also for the other cases already discussed, because of the same starting atomic configuration used. In the first two cases, however, such difference was progressively smoothed and it finally disappeared as a result of the atom displacement processes. In this case, instead, the dynamics of atomic species determined an amplification of the initial stoichiometry fluctuation and the formation of a surface domain of almost pure Ag at the vertex. This had a drastic effect on the dynamics of edge and surface species. Probably due to the favorable driving force to chemical demixing, Ag species exploring the surface gradually reached the Ag-rich vertex region and further enriched this and the neighboring regions. Starting from the vertex, the Ag-rich phase grew asymmetrically with respect to the nanorod axis and involved increasing portions of the system. An atomic configuration illustrating this situation is shown in Fig. 11. In this case, therefore, the dynamics of atomic species located at edges and surfaces promoted the separation of Ag- and Cu-rich phases already at relatively low temperatures. This proves that a spontaneous fluctuation of the relative concentration of atoms can promote an unexpected chemical evolution.

No significant difference between the dynamics occurred in simulations under gradual heating conditions and at 278 K was observed. The Ag surface domains gradually coalesced together and a single Ag-rich phase covered the Cu-rich bulk region of the nanorod. The 20-ns-long simulations showed that the atomic mobility at 278 K is high enough to allow the occurrence of the phase separation process mediated by cooperative atomic rearrangements. Of course, the higher the temperature, the higher the rate of such a process. However, even at 278 K a result analogous to the one obtained under gradual heating conditions can be attained on sufficiently long simulation times. The CSRO parameter Ω value attained at the end of the 20-ns-long simulations amounted indeed to about −0.70.

The dynamics of the nanorod containing a selected number of vacancies randomly distributed over the whole system volume is also very similar to the one already discussed. The presence of vacancies enhances the rate of atomic exchange processes in the bulklike region. It favors indeed the occurrence of conventional thermally-activated diffusion events. However, the impact of vacancies on the system dynamics is quite limited as a consequence of their gradual disappearance. From a total number of 100 vacancies introduced in the system at the beginning of the simulation, about 50 disappear within the first 6 ns as they attain the system surface. Twenty more disappear analogously within the successive 3 ns. It thus appears that vacancies annihilate at the surface after a fast diffusion within the bulklike nanorod interior. Their contribution to the atomic mobility is therefore negligible, at least within the explored time scale.

V. NANOWIRES WITH CONCENTRATION GRADIENTS

The occurrence of a phase separation process already at temperatures as low as 256 K, which are due to a local fluctuation in the relative content of Ag and Cu atoms, poses an intriguing question about the effects of concentration gradients on the stability of NSs. Such a question is investigated here in the case of the nanowire system. Indeed, the nanowire length allows the generation of suitable smooth concentration gradients.

The gradients were created at regular distances along the nanowire axis as shown in Fig. 1. The relaxed nanowire was ideally divided into eight roughly cubic portions by seven virtual planes perpendicular to the wire axis, which coincides with the z Cartesian direction. Two identical regions 0.5 nm wide were then defined on one side and the other of the virtual planes as shown in Fig. 12. The two regions form a 1-nm-wide zone that was divided again by virtual planes perpendicular to the wire axis into five domains. The number of Ag and Cu atoms within each domain was artificially modified by randomly selecting the desired number of Ag

and Cu atoms and transforming them into Cu and Ag species, respectively. The composition of the central domain is the richest in Ag or Cu atoms and the composition of the neighboring ones is arranged in order to obtain the smoothest possible concentration gradient. If a given central domain is, for example, Ag-rich, the central domains of adjacent zones will be Cu-rich and vice versa, as shown in Fig. 1. An Ag-rich region 1 nm wide is thus preceded and followed by Cu-rich regions of the same width. The central Ag-rich domains within each Ag-rich region were given the stoichiometries $Ag_{70}Cu_{30}$, $Ag_{80}Cu_{20}$, and $Ag_{90}Cu_{10}$. The Cu-rich ones were correspondingly given the stoichiometries $Ag_{30}Cu_{70}$, $Ag_{20}Cu_{80}$, and $Ag_{10}Cu_{90}$. The gradient g was then defined as the difference between the central domain composition and the $Ag_{50}Cu_{50}$ one. The g values, expressed in terms of units of molar fraction per unit of length, were equal to ± 0.4, ± 0.6, and ± 0.8 nm^{-1}.

The concentration gradients along the nanowire axis strongly influence the phase separation process. Not only is the rate of system decomposition significantly enhanced, but also the temperatures at which the phase separation occurs are different from the ones observed in previous cases. Concentration gradients seem indeed to favor the occurrence of collective atomic rearrangements in the bulklike regions of the nanowire at lower temperatures. The result is that already at about 270 K the $Ag_{50}Cu_{50}$ solid solution with gradients g equal to about ± 0.4 nm^{-1} has decomposed into Ag- and Cu-rich phases with about $Ag_{95}Cu_5$ and Ag_5Cu_{95} compositions. The arbitrarily chosen regular alternation of positive and negative gradient g values along the nanowire axis produced a corresponding regular modulation of the crystalline phases. A sketch of the nanowire after phase separation is shown in Fig. 13 for the sake of illustration.

The stability of the nanowire depends on the concentration gradients g along its axis. This was highlighted by analyzing the evolution of the CSRO parameter Ω as a function of the temperature. In this case, however, Ω was evaluated on a local basis in order to properly take into account the existence of concentration gradients. In particular, the CSRO parameter Ω was evaluated independently in each of the eight portions in which the nanowire was subdivided. The results are shown in Fig. 14. It can be seen that, although the temperature range within which Ω changes depends on the concentration gradient g, in all the cases Ω drops from about -0.08 to -0.76. The degree of phase separation attained at the end of the first stage of the phase separation process is therefore larger than in the absence of concentration gradients. Each trend was characterized by identifying the temperature at which the CSRO parameter Ω takes a value roughly in the middle of the drop, i.e., approximately -0.42. The eight temperature values obtained, one per nanowire portion, were then averaged to obtain the temperatures T_{sep} at which the phase separation process takes place. The average T_{sep} values are presented in Fig. 15 as a function of the concentration gradient g. It can be seen that the temperature T_{sep} decreases as the gradient g increases. Demixing is thus facilitated in the presence of concentration gradients and the system instability with respect to phase decomposition increases as the local deviation from the equiatomic composition increases.

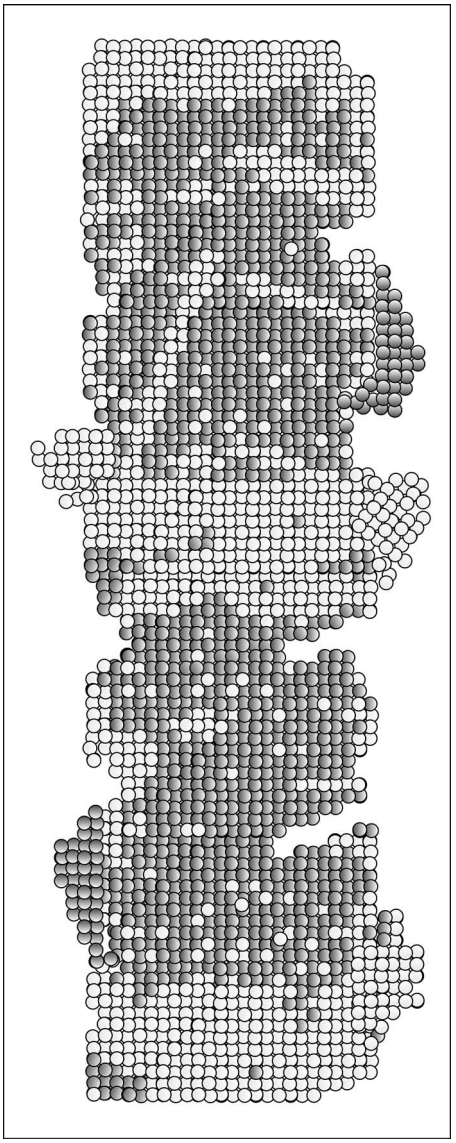

FIG. 13. A portion of the nanowire after phase separation. Data refer to the nanowire with gradients g equal to about ± 0.4 nm^{-1} at the temperature of 272 K. The light and dark gray circles indicate, respectively, Ag and Cu atoms.

The process of phase separation at temperatures as low as the observed T_{sep} ones is mostly governed by the mobility of surface species. However, significant collective atomic rearrangements take place in the bulklike regions. The predominance of individual surface displacements has two effects on the nanowire structure. The first one is directly evident from Fig. 13. The nanowire loses in fact its initial regular shape as a consequence of the disordered growth of the Ag- and Cu-rich domains, which proceeds via the continuous addition of atoms mostly from the surface. It is also worth noting that the crystalline structure can locally lose homogeneity. The formation of low-angle grain boundaries separating coherent fcc domains consequent to the individual atom displacement process is also expected. Their explicit identification is however complicated by the relatively disordered arrangement of the atomic species during the course of and after the decomposition process. Such identification has been possible in a

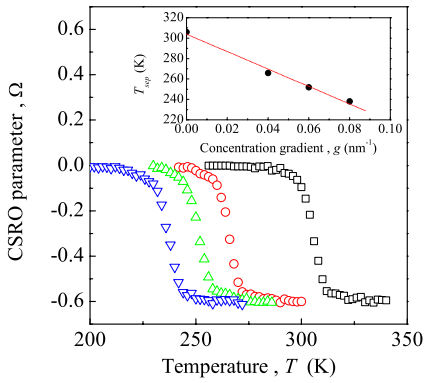

FIG. 14. (Color online) The CSRO parameter Ω of the nanowires with the concentration gradients g equal to 0 (□), ±0.4 (○), ±0.6 (△), and ±0.8 (▽)nm^{-1} as a function of the temperature T. The inset shows the temperature T_{sep} at which the phase separation occurs as a function of the concentration gradient g.

single case, with the grain boundary corresponding to a symmetric tilt (110) boundary. No evidence has been however obtained regarding the stability of such structure on relatively long simulation times. It is therefore possible that it could disappear as a consequence of the atomic displacements tending to lower the total energy of the nanowire system.

According to the configuration shown in Fig. 13, the nanowire structure seems to have been "eroded" by chemical etching processes. This is due to the relatively low temperatures at which the atomic displacements take place. Even though no specific calculation was performed, it is expected that the mechanical stability of the nanowire could be severely compromised.

The second effect of the predominance of surface atom displacements is that no definite surface segregation of Ag

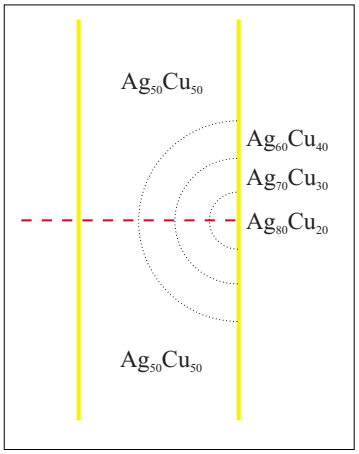

FIG. 15. (Color online) A schematic representation of the concentration gradient with a semicircular profile. The region involved in the gradient is about 1 nm wide along the nanowire axis. The vertical solid lines represent the edges of the nanowire. The horizontal dashed line represents the plane cutting the wire into two halves. The semicircular regions have the compositions reported on the side of the nanowire. The composition is elsewhere equal to $Ag_{50}Cu_{50}$.

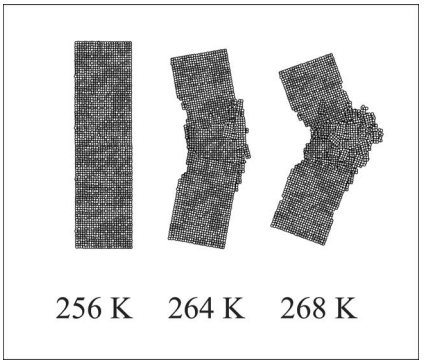

FIG. 16. A portion of the nanowire system with concentration gradient g equal to about +0.4 nm^{-1} characterized by a semicircular profile. The configurations refer to the quoted temperatures. The light and dark gray circles indicate, respectively, Ag and Cu atoms.

atoms is observed. Ag species do not tend to preferentially occupy the surface layers of the nanowire. Rather, the nanowire lowers its potential energy by promoting the decomposition of the metastable $Ag_{50}Cu_{50}$ alloy, thus forming separate Ag- and Cu-rich domains.

Aimed at further investigating the stability of nanowire systems in the presence of concentration gradients, additional simulations were carried out on a nanowire with a single concentration gradient located in the middle of its axis. In this case, however, the concentration gradient was no longer imposed perpendicular to the wire axis. As schematically shown in Fig. 16, the concentration gradient was generated with a semicircular profile. The concentration gradient g was set equal to about +0.4 nm^{-1}. The region involved by the concentration gradient is then Ag-rich.

The mechanism underlying the atomic mobility is similar to the one discussed in the previous case of concentration gradients perpendicular to the wire axis. The temperature range within which phase separation occurs is also similar. The structural response of the nanowire to the phase separation process is however remarkably different. In a sense, it can be regarded as an amplification of the disordering and "erosion" phenomena discussed above and illustrated by Fig. 13. It appears that individual and collective atomic displacements progressively induce a bending of the whole structure exactly in correspondence with the concentration gradient along the axis. The Ag atoms in the neighborhood of the region affected by the concentration gradient move toward it. This determines a disordered enrichment in Ag of such a region. The loss of Ag atoms undergone by the neighboring regions is not immediately contrasted by the diffusion of Cu species as a consequence of the low temperatures, so that a net flow of atoms takes place. The nanowire therefore undergoes first a distortion and then a bending. These are probably due to the disordered migration of atomic species, the consequent formation of adjacent coherent domains separated by low-angle grain boundaries and the attempt of lowering the system energy by eliminating such boundaries by a rotation of coherent domains. Further analyses are, however, needed to properly investigate this point and support the results of the present preliminary phenomenological study.

VI. CONCLUSIONS

The present work provides a detailed account of the thermal responses of nanometer-sized rods and wires consisting of a metastable $Ag_{50}Cu_{50}$ crystalline solid solution. Due to the positive enthalpy of mixing between Ag and Cu, the systems undergo a phase separation process. In the case of homogeneous composition, such a process takes place roughly in two stages. In the first one, atomic mobility is essentially due to individual displacements of edge and surface atoms. Under such circumstances, demixing proceeds by forming Ag- and Cu-rich domains at the plane surfaces of the rod and wire systems. During this stage, at least within the time scales explored, the number of Ag- and Cu-rich surface domains seems to be in dynamic equilibrium. The equilibrium is, however, broken at temperatures above 260 K in favor of Ag-rich domains. This marks the transition from the first to the second stage of phase separation, when extended surface segregation phenomena determine the formation of structures with the Ag-rich phase entirely covering the surfaces. Atomic mobility is here governed by cooperative rearrangements, which are responsible for the diffusion of Ag atoms from bulklike to surface regions. Despite the deep reorganization of the chemical order, all the systems keep their initial regular shape. This no longer occurs when nanowires with concentration gradients are considered. In these cases the phase separation process proceeds at lower temperatures, promoting the formation of separate Ag- and Cu-rich domains. In addition, the migration of surface species produces a considerable distortion of the initial shape and, in the case of concentration gradients parallel to the wire axis, also a bending of the structure.

The numerical findings collected in the present work therefore show that the stability of nanorods and nanowires formed by metastable phases is intimately connected with the chemical order. Far from being conclusive, the results obtained define for the systems investigated a relatively complex conceptual framework. Only approximate mechanistic inferences have been obtained from the present simulations, whereas a more systematic and deeper investigation is needed to shed light on the fine details of the atomic-scale processes underlying the phase separation.

ACKNOWLEDGMENTS

Financial support was given by the University of Cagliari and Trinity College Dublin. A. Ermini, ExtraInformatica s.r.l., is gratefully acknowledged for his kind assistance and support.

*Corresponding author; delogu@dicm.unica.it

[1] P. Moriarty, Rep. Prog. Phys. **64**, 297 (2001).
[2] J. Jortner C. N. R. Rao, Pure Appl. Chem. **74**, 1491 (2002).
[3] G. A. Ozin and A. Arsenault, *Nanochemistry: A Chemical Approach to Nanomaterials* (RSC, Cambridge, UK, 2005).
[4] D. Chandler, *Introduction to Modern Statistical Mechanics* (Oxford University Press, Oxford, UK, 1987).
[5] Q. S. Mei and K. Lu, Prog. Mater. Sci. **52**, 1175 (2007).
[6] Special issue on Nanowires, edited by Y. Xia and P. Yang, Adv. Mater. **15**(5), 341-468 (2003).
[7] C. N. R. Rao and A. Govindaraj, *Nanotubes and Nanowires* (RSC, Cambridge, UK, 2005).
[8] *Handbook of Theoretical and Computational Nanotechnology*, edited by M. Rieth and M. Schommers (American Scientific, New York, 2005).
[9] E. Rabkin and D. Srolovitz, Nano Lett. **7**, 101 (2007).
[10] *Smithells Metals Reference Handbook*, 7th ed., edited by E. A. Brandes and G. B. Brook (Butterworth-Heinemann, Oxford, 1992).
[11] W. L. Johnson, Prog. Mater. Sci. **30**, 81 (1986).
[12] R. Busch, F. Gartner, C. Borchers, P. Haasen, and R. Bormann, Acta Mater. **44**, 2567 (1996).
[13] M. Athenes, P. Bellon, and G. Martin, Acta Mater. **48**, 2675 (2000).
[14] C. Suryanarayana, Prog. Mater. Sci. **46**, 1 (2001).
[15] Y. Sun and Y. Xia, Science **298**, 2176 (2002).
[16] G. S. Metraux, Y. C. Cao, R. Jin, and C. A. Mirkin, Nano Lett. **3**, 519 (2003).
[17] Y. Sun and Y. Xia, J. Am. Chem. Soc. **126**, 3892 (2004).
[18] E. Hao, S. Li, R. C. Bailey, S. Zou, G. C. Schatz, and J. T. Hupp, J. Phys. Chem. B **108**, 1224 (2004).
[19] Y. Vasquez, A. K. Sra, and R. Schaak, J. Am. Chem. Soc. **127**, 12504 (2005).
[20] A. M. Schwartzberg, T. Y. Olson, C. E. Talley, and J. Z. Zhang, J. Phys. Chem. B **110**, 19935 (2006).
[21] V. Rosato, M. Guillope, and B. Legrand, Philos. Mag. A **59**, 321 (1989).
[22] F. Cleri and V. Rosato, Phys. Rev. B **48**, 22 (1993).
[23] G. Mazzone, V. Rosato, M. Pintore, F. Delogu, P. F. Demontis, and G. B. Suffritti, Phys. Rev. B **55**, 837 (1997).
[24] H. C. Andersen, J. Chem. Phys. **72**, 2384 (1980).
[25] S. Nosè, J. Chem. Phys. **81**, 511 (1984).
[26] M. Parrinello and A. Rahman, J. Appl. Phys. **52**, 7182 (1981).
[27] M. P. Allen and D. Tildesley, *Computer Simulation of Liquids* (Clarendon, Oxford, 1987).
[28] G. E. Tommei, F. Baletto, R. Ferrando, R. Spadacini, and A. Danani, Phys. Rev. B **69**, 115426 (2004).
[29] J. D. Honeycutt and H. C. Andersen, J. Phys. Chem. **91**, 4950 (1987).
[30] J. R. Morris, Phys. Rev. B **66**, 144104 (2002).
[31] J. R. Morris and X. Song, J. Chem. Phys. **116**, 9352 (2002).
[32] C. Donati, J. F. Douglas, W. Kob, S. J. Plimpton, P. H. Poole, and S. C. Glotzer, Phys. Rev. Lett. **80**, 2338 (1998).
[33] N. Giovambattista, S. V. Buldyrev, H. E. Stanley, and F. W. Starr, Phys. Rev. E **72**, 011202 (2005).
[34] H. Zhang, D. J. Srolovitz, J. F. Douglas, and J. A. Warren, Phys. Rev. B **74**, 115404 (2006).
[35] A. C. Lund and C. A. Schuh, Phys. Rev. Lett. **91**, 235505 (2003).
[36] A. C. Lund and C. A. Schuh, J. Appl. Phys. **95**, 4815 (2004).
[37] S. Odunuga, Y. Li, P. Krasnochtchekov, P. Bellon, and R. S. Averback, Phys. Rev. Lett. **95**, 045901 (2005).

[38] F. Delogu, Nanotechnology **18**, 235706 (2007).
[39] H. Mori, M. Komatsu, K. Takeda, and H. Fujita, Philos. Mag. Lett. **63**, 173 (1991).
[40] H. Yasuda and H Mori, Z. Phys. D: At., Mol. Clusters **31**, 131 (1994).
[41] F. Baletto, C. Mottet, and R. Ferrando, Phys. Rev. B **66**, 155420 (2002).
[42] F. Baletto and R. Ferrando, Rev. Mod. Phys. **77**, 371 (2005).
[43] M. J. Mehl and D. A. Papaconstantopoulos, Phys. Rev. B **54**, 4519 (1996).
[44] L. A. Braunstein, S. V. Buldyrev, S. Havlin, and H. E. Stanley, Phys. Rev. E **65**, 056128 (2002).
[45] F. Baletto, C. Mottet, and R. Ferrando, Phys. Rev. Lett. **90**, 135504 (2003).